Zabouri Abdelhamid [1], Chenafa Mohamed [1], Naima khalfallah [1], Bendjeddou Yacine [2], Kacimi Abderrahmen [3], Mourad Boufadene [4]

Department of electrical engineering, national polytechnic High school, Automation laboratory and systems analysis (LAAS), maurice audin-oran BP 1523 el'm'naouer,oran, (Algeria)(1).
Département de Génie Electrique, Ecole Supérieure en Génie Electrique et Energétique d'Oran, Laboratoire de Génie Electrique et Matériaux, 31000 Bir El Djir, (Algeria) (2).
Department of electrical engineering, Automation laboratory and systems analysis (LAAS), Institute of Maintenance and Industrial Safety, University of Oran 2 Mo-hamed Ben Ahmed, B.P 170, ElM'Naouer 31000, Oran (Algeria) (3).
Department of Electrical Engineering, High School of Applied Science (ESSA), Lycee Emir Abdelkqder Bab El Oued, (Alger) (4).

doi:10.15199/48.2023.11.28

DC-Bus Voltage Control of Self-Excited Induction Generator for Variable-Speed Wind Turbine Generation Including Dynamic Saturation

Abstract. *The presented paper proposes a linear polynomial controller that demonstrates robustness against parameter uncertainties when used for voltage-oriented control of the id and iq currents in a squirrel cage induction generator. The control approach maintains generated voltage at a steady-state regime, even in the presence of disturbances, through the identification of the magnetic curve. The controller's efficacy is evaluated under various speed and load torque variations through simulation using MATLAB/SIMULINK. The obtained results highlight the effectiveness of the proposed approach in improving wind turbine efficiency, making it a promising solution for DC micro grid applications.*

Streszczenie. *W prezentowanej pracy zaproponowano liniowy wielomianowy regulator, który wykazuje odporność na niepewność parametrów, gdy jest używany do zorientowanego na napięcie sterowania prądami id i iq w klatkowym generatorze indukcyjnym. Podejście kontrolne utrzymuje generowane napięcie w stanie ustalonym, nawet w obecności zakłóceń, poprzez identyfikację krzywej magnetycznej. Skuteczność sterownika jest oceniana przy różnych zmianach prędkości i momentu obciążenia poprzez symulację przy użyciu MATLAB/SIMULINK. Uzyskane wyniki podkreślają skuteczność proponowanego podejścia w poprawie wydajności turbin wiatrowych, co czyni je obiecującym rozwiązaniem dla zastosowań w mikrosieciach prądu stałego. (**Sterowanie napięciem szyny DC samowzbudnego generatora indukcyjnego do generacji turbin wiatrowych o zmiennej prędkości, w tym dynamiczny Nasycenie)***

Keywords: RST Robust, SESC-IG, PLL, PI controller.
Słowa kluczowe: RST Robust, SESC-IG, PLL, PI kontroler.

Introduction

Renewable energies have emerged as a promising solution for generating electrical energy from renewable sources, such as wind turbines, solar radiation, and water cycles. In particular, wind energy has been the focus of significant research efforts since James Blyth's discovery of wind turbines in 1888 in Scotland. Researchers have focused on developing more efficient wind turbines to increase energy production and capacity [1].

A functional prototype of a bladed wind turbine was successfully tested in the early stages of 1941. Amongst the various generator types available, the self-excited squirrel cage induction generator (SESC-IG) has gained wide popularity owing to its robust construction, low maintenance costs, affordability, and its ability to operate seamlessly in overload and short circuit scenarios [2]. However, the SESC-IG requires shunt capacitors in the circuit to produce the reactive power, and the difference between the power needed for the load and the machine in conjunction with the shunt capacitors results in poor voltage regulation, limiting its efficiency.

To address this issue, power converters (AC-DC) are used to provide the desired power conditions, regardless of the external input load. However, controlling the converters has been a challenge for many researchers, and several control techniques have been proposed to control the power and reduce harmonic distortion. In [3-4], the authors used the technique of indirect Field oriented control (IFOC) to separate the control of quantities such as currents and voltages of the direct axis with the quadrature axis. In [5], the Electromagnetic Frequency Regulator (EFR) technique was used to control the rotor speed by reaching a desired frequency value, while in [6], state estimation was preferred over sensors, which can be fragile and vulnerable to damage during operation. Direct torque control (DTC), known for its advantage of controlling the motor in variable frequency, was used in [7]. Other control techniques were proposed in [8-9].

In this paper, we propose a voltage-oriented control (VOC) technique to control the active and reactive power, respectively, by controlling the direct and quadratic currents (Id, Iq) and the DC bus voltage. This technique relies on estimating the position theta using the phase-locked loop (PLL) approach [10]. Previous researchers have employed similar techniques, such as integrating the maximum power point tracking (MPPT) technique to control speed and estimate the desired DC bus voltage [11] and using VOC with sliding mode controller to control currents [12].

Our work focuses on replacing the current controller with a linear polynomial controller, known as robust reference signal tracking (RST). RST is a linear controller technique that provides a phase margin of 90 and an infinite gain margin while effectively managing the trade-off between performance and robustness.

We extract the parameters of the generator using the classical method of identification based on short circuit and no-load tests [13] while taking into account the phenomenon of saturation of their magnetic circuit with a simple and precise method, as the amplitude of the voltage generated by this machine is entirely affected by the magnetization curve [14].

This paper is organized as follows. In Section 1, we present the model of the SESC-IG. In Section 2, we describe the identification of the magnetization curve. In Section 3, we discuss the VOC control, and in Section 4, we explain the RST control. In Section 5, we present the simulation results with their interpretation. Finally, we conclude with a summary and discussion in Section 6.

Model of asynchronous squirrel C age Induction Generator (SCIG)

The behavior of an induction generator has been described with a dynamical equation based on an equivalent circuit [15] shown in (Fig 1).

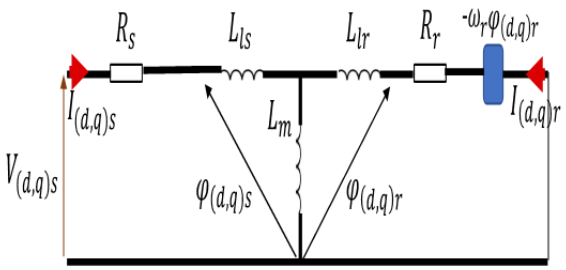

Fig.1. The d,q model of the SEIG in the stationary frame of reference

$$\frac{dI_{qs}}{dt} = \left(\frac{1}{k}\right)\begin{pmatrix} -L_r R_s I_{qs} - L_m{}^2 I_{ds} + L_m R_r I_{qr} \\ -L_m L_r \omega_r I_{dr} - L_r V_{qs} - L_m V_{qr} \end{pmatrix} \tag{1}$$

$$\frac{dI_{ds}}{dt} = \left(\frac{1}{k}\right)\begin{pmatrix} -L_m{}^2 I_{qs} - L_r R_s I_{ds} + L_m L_r \omega_r I_{qr} \\ -L_m L_r I_{dr} - L_r V_{ds} - L_m V_{dr} \end{pmatrix} \tag{2}$$

$$\frac{dI_{qr}}{dt} = \left(\frac{1}{k}\right)\begin{pmatrix} L_m R_s I_{qs} + L_s \omega_r I_{ds} - L_s R_r I_{qr} \\ + L_s L_r \omega_r I_{dr} + L_m V_{qs} - L_s V_{qr} \end{pmatrix} \tag{3}$$

(4)

$$\frac{dI_{dr}}{dt} = \left(\frac{1}{k}\right)\begin{pmatrix} -L_s L_r \omega_r I_{qs} + L_m R_s I_{ds} - L_s \omega_r I_{qr} \\ -L_s R_r I_{dr} + L_m V_{ds} - L_s V_{dr} \end{pmatrix}$$

$$\frac{dV_{qs}}{dt} = \left(\frac{1}{C}\right) I_{qs} \tag{5}$$

$$\frac{dV_{ds}}{dt} = \left(\frac{1}{C}\right) I_{ds} \tag{6}$$

where: $I_{qs}, I_{ds}, I_{qr}, I_{ds}$ – are the stator and rotor currents respectively in the mode DQ. L_m – the magnetizing inductance. $L_s L_r$– the stator and rotor inductance respectively. R_s, R_r– the resistances of the stator and rotor windings. V_{qs} , V_{ds} – the voltages in the model DQ. V_{qr}, V_{dr} – the residual flux tensions, the ω_r – is the electrical speed. c – is the value of the capacitor.

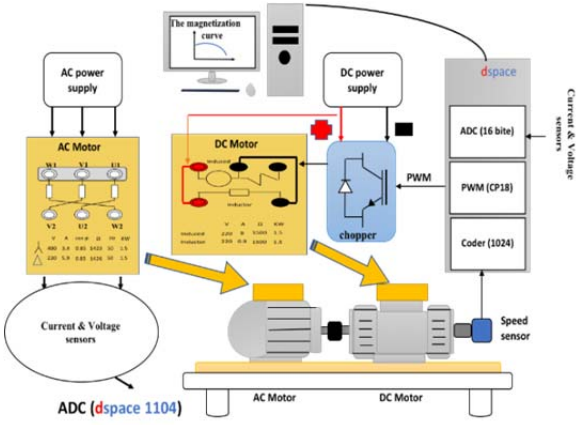

Fig.2. Global diagram of the principle of determination of the magnetization curve

The extraction of the magnetization curve

As highlighted in the introduction, the dynamic voltage behavior is determined by the magnetization curve. To obtain this curve, a Synchronous Velocity Test was performed by controlling a prime mover (DC motor) to run at a constant speed of 1500 rpm, resulting in zero slip [14]. (Fig 2) illustrates the method used to determine this cu

In (Fig 3), the mutual inductance is calculated during the Synchronous Velocity Test as follows:

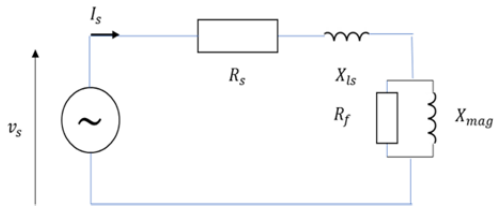

Fig.3. Equivalent circuit of the Synchronous Velocity Test

$$X_{mag} = L_m \omega \rightarrow L_m = \frac{V_s}{I_s \omega} \tag{7}$$

$$V_s = \sqrt{V_{\alpha s}{}^2 + V_{\beta s}{}^2} \tag{8}$$

$$I_s = \sqrt{I_{\alpha s}{}^2 + I_{\beta s}{}^2} \tag{9}$$

$$\omega = 2\pi f \tag{10}$$

Fig.4. Experimental setup

Control of DC Motor

To control the dc motor it is necessary to identify its physical parameters and since this system is mono-variable we can identify it by the way of attacking this system by an input signal (step or signal frequency-rich) and see their behavior in terms of output Speed, the result of the ratio between the input-output signals gives us a transfer function which contains the physical parameters of the machine. The handling of this idea is done by software (MATLAB/Simulink) by the ident tools application as shown in (Fig 5):

a)

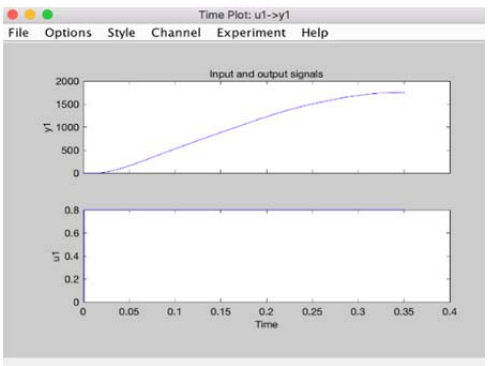

b)

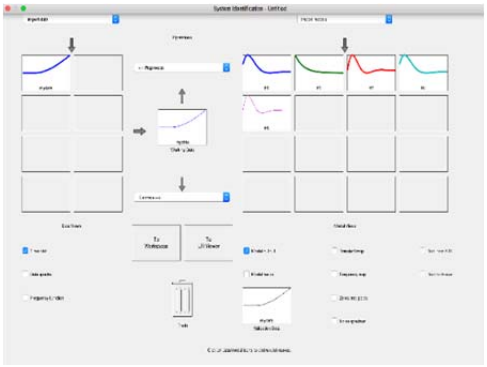

c)

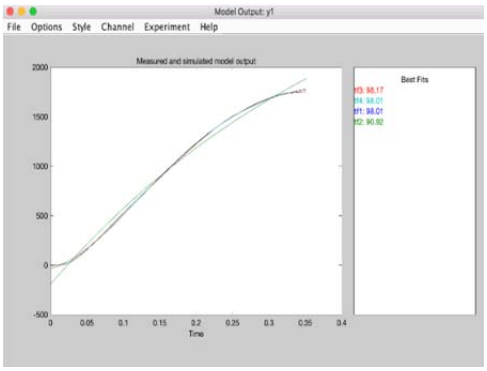

d)

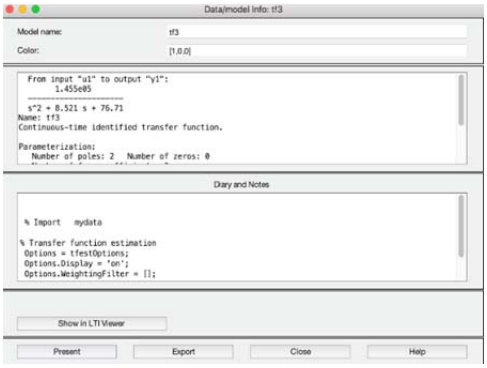

Fig.5. The method of identification of the parameters of the system (DC motor)

Discussion of the identification method

In this section, we imported two input/output signal vectors (Fig 5a) and measured the output signal through the encoder sensor (Fig 2). These signals were then saved using software control desk in the ident-tools application (Figure 5b) to determine the transfer function. We selected two poles without zeros, which gave a good percentage of 98.17 (red curve) as shown in (Fig 5c). Based on this transfer function, we calculated the corrector using a PI controller (Fig 6). (Fig 6) shows the closed loop of the correction.

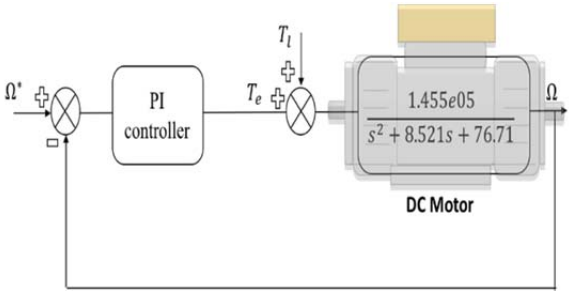

Fig.6. Speed control loop

Polynomial identification of the magnetization curve

In this section, we have utilized Equation (7) to identify the polynomial of the magnetization curve, as illustrated in (Fig B7). The curve was obtained by varying the applied voltage and magnetization current, which is shown in (Fig 7) below.

The polynomial function that describes the magnetization curve has been obtained with Curve Expert Professional software.

$$L_m = -(1.1118e-10)V_s^4 + (9.7452e-8)V_s^3 - (3.2047e-5)V_s^2 + (0.0041201)V_s + 0.556 \quad (11)$$

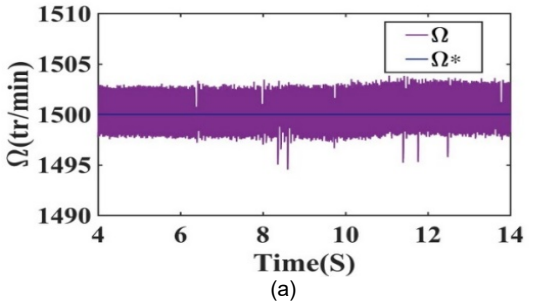

(a)

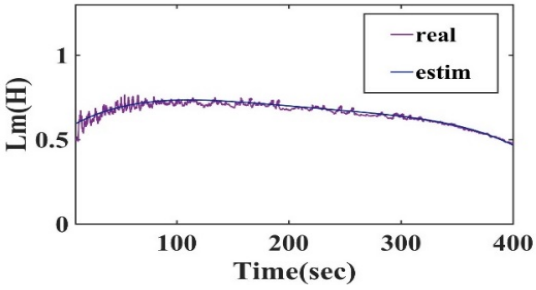

(b)

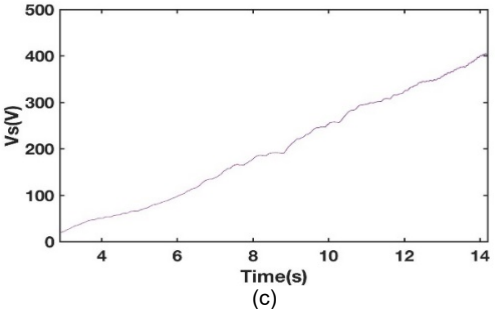

(c)

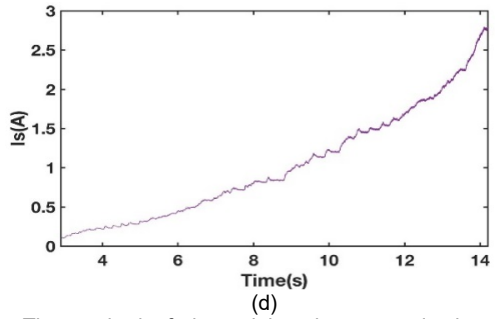

(d)

Fig .7. The method of determining the magnetization curve, a: Comparison between the reference rotor speed and the actual measurement, b: The magnetization curve as a function of voltage, c: The applied voltage (Vs), d: The magnetization current (Is)

We integrated a polynomial function instead of a constant L_m in the model of the SCIG. As a result, in the simulation of the SESC-IG, we obtained a good agreement between the voltage accumulation results shown in (Fig 8a)

and the experimental results shown in (Fig 8b) at a constant speed of 1600 rpm and with a capacitance value of 30μF.

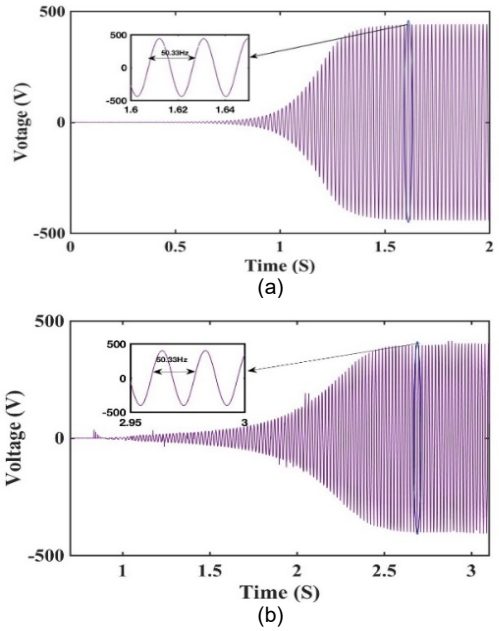

Fig .8. Voltage accumulation in a self-excited induction generator, a: simulation result, b: experimental result

The voltage-oriented control (VOC)

The global diagram of the voltage-oriented control is presented in the following figure:

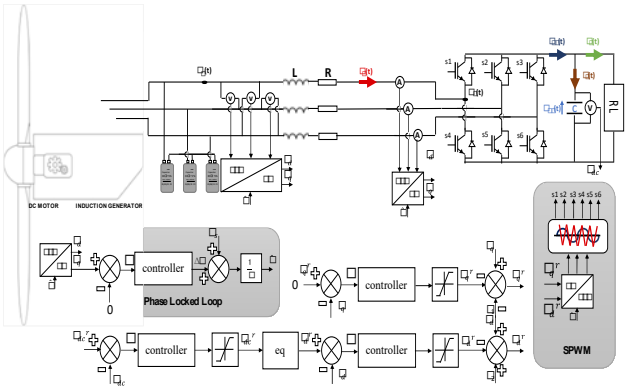

Fig 9. Global diagram of the VOC control technique

The underlying principle of the VOC control strategy is founded on Kirchhoff's theory. Within (Fig 9), the blue rectangle showcases the utilization of Kirchhoff's rule, which can be expressed as follows

$$(12)\quad e_{abc}(t)-V_{abc}(t)=L\frac{dI_{abc}(t)}{dt}+RI_{abc}(t)$$

Applying Laplace transformation to Equation (12) yields:

$$(13)\quad e_{dq}(t)-V_{dq}(t)=L\frac{dI_{dq}(t)}{dt}+RI_{dq}(t)$$

$$(14)\quad V_d(t)=e_d(t)-L\frac{dI_d(t)}{dt}-RI_d(t)+L\omega_r I_q(t)$$

$$(15)\quad V_q(t)=e_q(t)-L\frac{dI_q(t)}{dt}-RI_q(t)+L\omega_r I_d(t)$$

$$(16)\quad V_d(t)=e_d(t)-LsI_d(t)-RI_d(t)+L\omega_r I_q(t)$$

$$(17)\quad V_q(t)=e_q(t)-LsI_q(t)-RI_q(t)+L\omega_r I_d(t)$$

(18)

$$U_d{}^r(s)=LsI_d(s)+RI_d(s)=e_d(s)+L\omega_r I_q(s)-V_d(s)$$

(19)

$$U_q{}^r(s)=LsI_q(s)+RI_q(s)=e_q(s)+L\omega_r I_d(s)-V_q(s)$$

$$(20)\quad I_d(s)=\frac{1}{Ls+R}U_d^r(s)$$

$$(21)\quad I_q(s)=\frac{1}{Ls+R}U_q^r(s)$$

In the red circle of (Fig 9) the Kirchhoff law yields:

$$(22)\quad I_c(t)=I_{dc}(t)-L_L(t)=C\frac{dV_{dc}(t)}{dt}$$

$$(23)\quad I_c(s)=R_lI_{dc}(s)-V_{dc}(s)=R_lCsV_{dc}(s)$$

$$(24)\quad V_{dc}(s)=\frac{R_l}{R_lCs+1}I_{dc}(s)$$

The mathematical development of the voltage-oriented control (VOC) can be expressed as:

$$(25)\quad P(t)=\frac{3}{2}e_d(t)I_d(t)$$

$$(26)\quad P(t)=V_{dc}(t)I_{dc}(t)$$

$$(27)\quad I_d^r(t)=\frac{3}{2}\frac{V_{dc}(t)}{e_d(t)}I_{dc}{}^r(t)$$

$$(28)\quad I_q^r(t)=0$$

$$(29)\quad V_d{}^r(t)=e_d(t)-U_d{}^r(t)+L\omega_r I_q(t)$$

$$(30)\quad V_q{}^r(t)=e_q(t)-U_q{}^r(t)+L\omega_r I_d(t)$$

The voltage $V_{(d,q)}$, and the current $I_{(d,q)}$ are determined using a park transformation with Theta position estimated by the PLL technique, The Phase-loop-locked rectangle in the global diagram shows the method for estimating this Theta [10].

The voltage and currents controllers

The basis of the VOC control lies in the correction of the currents $I_{(d,q)}$ and the voltage V_{dc} as a result.

The voltage and currents controllers

To find the current $I_{(d,q)}$you have to control the voltage V_{dc}

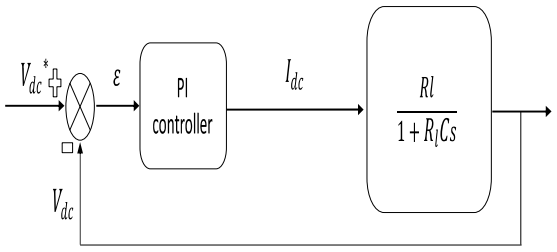

Fig 10. Closed loop regulation of the DC-bus voltage by PI corrector

(Fig 10) shows the general structure of the voltage regulation V_{dc} which is controlled via a PI controller and the system which is determined with the help of the orange circle in (Fig 9), The gains (K_p, K_i) (proportional-integrator) of the PI Controller are calculated using the pole placement method.

Current Regulation $I_{(d,q)}$

To find the voltages $U_{(d,q)}$respectively the currents $I_{(d,q)}$respectively must be controlled

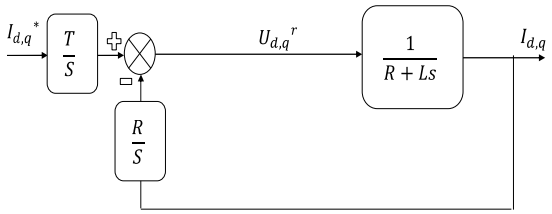

Fig.11.Closed loop regulation of the current $I_{(d,q)}$by the RST

RST polynomials are utilized to manage the output of a dynamic system by setting it to a desired input reference through pole placement synthesis or the matrix method mentioned in [16]. However, the performance of this method is suboptimal in situations where the system's parameters vary. In response to this issue, Professor Philippe de Larmina in automation has devised a technique to convert the RST controller into a robust controller. This enhanced controller can handle parameter uncertainties and adapt to changes in the parameter margin by adding a feedback loop and designing a compensator. The new method offers a more reliable and robust controller that can operate even in situations where the system's parameters fluctuate.

We put a polynomial equation $p(s)$ that will be factorized into two factors equation $F(s)$and equation $C(s)$ which are the dominant auxiliary polynomial, respectively:

$$P(s) = F(s)C(s) \quad (31)$$

Our open-loop system $G(s)$ is written as follows:

$$G(s) = \frac{B(s)}{A(s)} \quad (32)$$

$$\begin{cases} B(s) = [0 \quad 1] \\ A(s) = [L \quad R] \end{cases} \quad (33)$$

The closed-loop system becomes:

$$\frac{I_d}{I_d^*} = \frac{B(s)T(s)}{A_i(s)S1(s) + B(s)R(S)} \quad (34)$$

$$P(s) = A_i(s)S1(s) + B(s)R(S) \quad (35)$$

$$A_i(s) = sA(s) \quad (36)$$

The solution of the Bezout Equation (35) is used to determine the polynomials $R(s), S(s), T(s)$ of the corrector.

The LQG/LTR technique have been used in [17], this technique allows us to minimize the norm of the sensitive function $\left[\frac{A_i(s)}{F(s)} - \mathbf{1}\right]$ to find a dominant horizon $[T_o < 1]$ this method gives us a better margins module and delay, respectively. The auxiliary horizon $T_c$isobtained by minimizing the following function $[\frac{B(s)}{C(s)} - \mathbf{1}]$, therefore, the approximation values of $T_o$and T_c are obtained from $A(s)$ and $B(s)$ respectively.

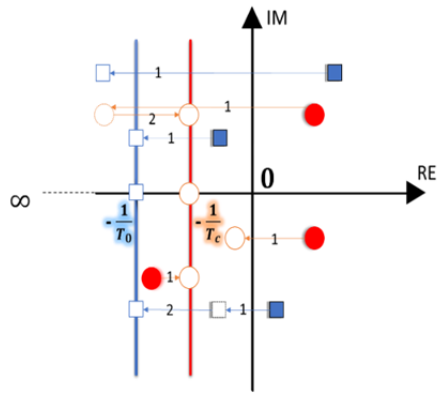

Fig 12. The investment strategy of horizons T_o,T_c

Where

Open-loop poles. Dominant poles.
Open loop zeros Accessory poles

A djustment Principle

The objective is to set the T_o to the right side and $T_c$to the left side of the complex plain, the restoration factor $KC = \frac{T_o}{T_c}$ is used to achieve a good trade-off between performance and robustness, however, by increasing the value of $T_o$the delay margin increased and therefore, we lose the performance. the (Fig 12) below shows the principle.

Results and discussion

The control simulation (VOC) was performed using MATLAB/Simulink. The machine's parameters used in this study are listed in the Appendix. The active power is generated by $1.5\,kW$ and the reactive power by a $30\,\mu F$ capacitor, while the DC bus voltage was successfully controlled despite a variation in speed, as shown in (Fig 13 e), and a disturbance in the resistive load, which changed from $400\,ohms$ to $160\,ohms$ at $T = 6\,sec$, as seen in (Fig 13a). The regulation of the DC bus voltage was referenced to maintain a value of 800 volts, and the regulation of currents $I_{(d,q)}$ controlled the active and reactive power, respectively, in accordance with the theory of (VOC).

The results of the current regulation are shown in (Fig 13b), with the corresponding control signals in (Fig 13f), which are well-filtered due to the RST Corrector's good load specifications. A good compromise between performance and robustness was achieved, resulting in satisfactory margins (phase, gain), as indicated in (Fig 13g).

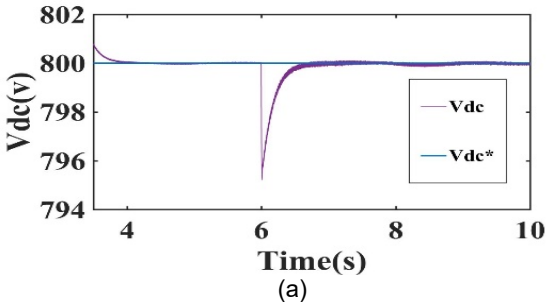

(a)

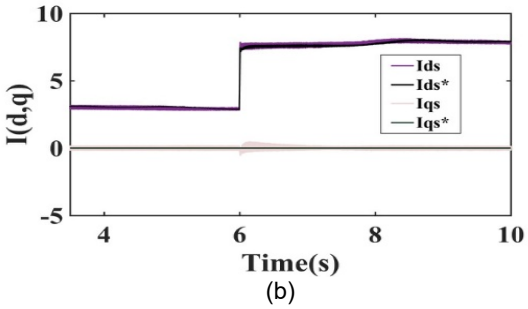

(b)

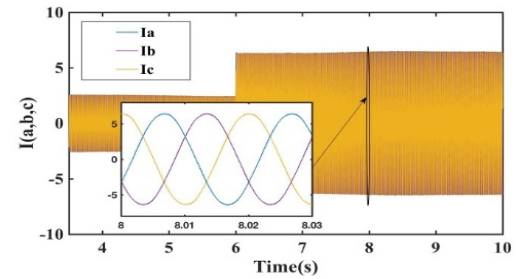

(c)

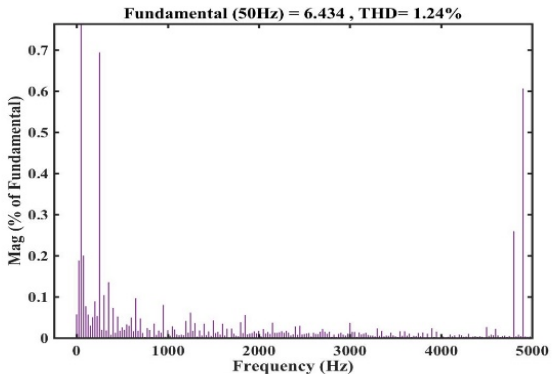

(d)

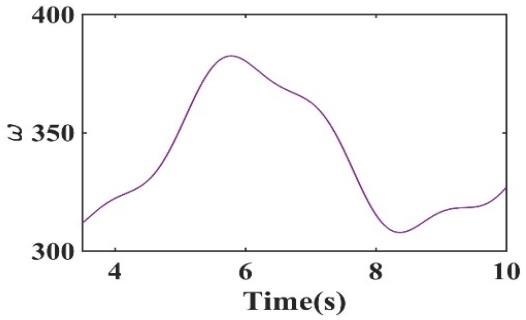

(e)

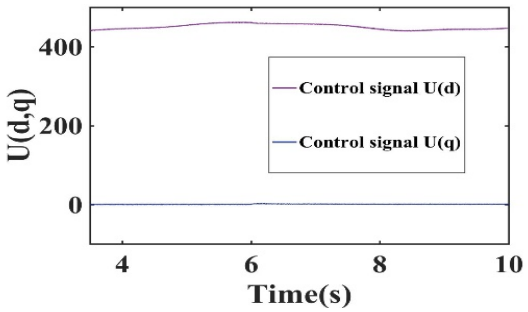

(f)

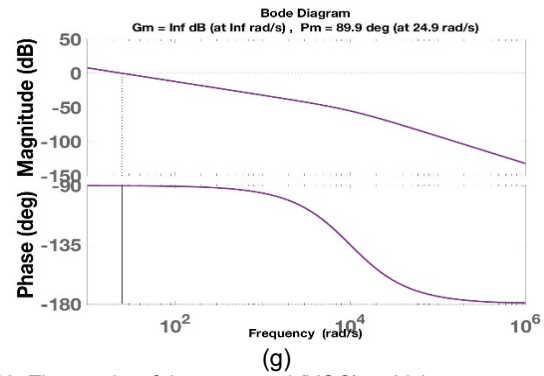

(g)

Fig 13. The results of the command (VOC), a: Voltage V_{dc}control, b: Current $I_{(d,q)}$control, c: Stator current, d: Harmonic spectra of the stator current, e: Rotor speed, f: control signal $U_{(d,q)}$, g: bode diagram of Current control

Conclusion

The present study introduces an RST controller for a squirrel cage induction generator, with the objective of regulating the I_d and $I_q$currents to attain the desired active and reactive powers. To this end, the mutual inductance, rotor inductance, and stator inductance parameters were identified using the magnetic curve. The outcomes of this research showcase the effectiveness of the proposed approach in accomplishing the aforementioned control objectives. The RST controller put forth in this study can be deemed as a robust and reliable solution for regulating squirrel cage induction generators. Further research can explore the optimization of the proposed method and its application in other types of generators.

Appendix

Table 1. Asynchronous motor parameters with controller gains.

parameters	Values
Rated power	$1.5Kw$
Rated voltage	$400volt$
Rated speed	$1423rpm$
Rated frequency	$50Hz$
Stator resistance	4.83Ω
Rotor resistance	3.19Ω
Mutual inductance	$0.51H$
Pair number of poles	2
Kp	1.49
Ki	17.67
$\frac{1}{T_o}$	0.09
$\frac{1}{T_c}$	$1e-4$

Nomenclature

$V_{(d,q)}$: The line voltages in frame D, Q
$I_{(d,q)}$: The line currents in reference to D, Q.
$U_{(d,q)}$: The control signals that have come out of regulation of the currents.
I_c, I_l: The capacity current, load current.
V_{dc}, I_{dc}: The dc-bus voltage, dc-bus current.
Kp, Ki: The proportional, integrator PI corrector gains.
$R(s), S(s), T(s)$: Are polynomials of the RST corrector.
$B(s), A(S)$: The numerator denominator of system respectively.
$F(s), C(s)$: The desired polynomial factor of RST corrector
$1/To, 1/Tc$: The horizons of the desired poles of RST corrector.

ACKNOWLEDGMENT

This Works is supported by the: Direction Générale de la Recherche Scientifique et du Développement Technologique (DGRSDT).

Authors

phd student zabouri Abdelhamid ENP-Oran Email: zabouri.2018@gmail.com, pr chenafa Mohamed ENP-Oran Email: mchenafa@yahoo.fr , DR Naïm KHALFALLAH ENP-Oran Email: Naïma.khalfallah@enp- oran.dz, DR bendjeddou yacine Higher School of Electrical and Energetic Engineering of Oran Email: yacineunivers@yahoo.fr , DR kacimi abderrahmane ,IMSI-Oran Emai:Kdjoujou@gmail,com, DR Mourad Boufadene High School of Applied Science (ESSA)Email: morinelec@yahoo.fr

REFERENCES

[1] Yang, Han, Jin Chen, and Xiaoping Pang. "Wind turbine optimization for minimum cost of energy in low wind speed areas considering blade length and hub height." Applied Sciences 8.7 (2018): 1202.

[2] Ghanim, Ammar Shamil, and Ahmed Nasser B. Alsammak. "Modelling and Simulation of Self-Excited Induction Generator Driven by a Wind Turbine." Восточно-Европейский журнал передовых технологий 6.8 (2020) : 6-16.

[3] Domínguez-García, José Luis, et al. "Indirect vector control of a squirrel cage induction generator wind turbine." Computers & Mathematics with Applications 64.2 (2012): 102-114.
[4] Bašić, Mateo, Dinko Vukadinović, and Miljenko Polić. "Fuzzy DC-voltage controller for a vector controlled stand-alone induction generator." order 1 (2013): 2.
[5] Ramos, Thales, et al. "Slip control of a squirrel cage induction generator driven by an electromagnetic frequency regulator to achieve the maximum power point tracking." Energies 12.11 (2019): 2100.
[6] Bašić, Mateo, et al. "Sensorless maximum power control of a stand-alone squirrel-cage induction generator driven by a variable-speed wind turbine." Journal of Electrical Engineering & Technology 16 (2021): 333-347
[7] Abdelli, Radia, et al. "Application and Comparison of Different Control Strategies of Induction Generator in Wind Energy Conversion System." 2019 7th International Renewable and Sustainable Energy Conference (IRSEC). IEEE, 2019.
[8] Oussama Abdessemad, Ahmed Lokmane Nemmour, Lamri Louze, Abdelmalek Khezzar (2021), 'Real-Time Implementation of a Novel Vector Control Strategy for a Self-Excited Asynchronous Generator Driven by a Wind Turbine', journal européenne des systèmes automatisés, vol.54, No. 2, pp.235-241.
[9] Mohammed M. Khalaf, Amer M. Ali (2021), 'PERFORMANCE AS-SESS OF SELF-EXCITED IG DRIVEN BY WIND TURBINE WORKING WITH FC-TCR', Journal of Engineering and Sustainable Development, Vol. 25, No. 05, pp. 2520-0917.
[10] Xiong, Liansong, et al. "PLL-Free Voltage Oriented Control Strategy for Voltage Source Converters Tied to Unbalanced Utility Grids." Frontiers in Energy Research (2022): 806.
[11] Amieur, Toufik, Djamel Taibi, and Oualid Amieur. "Voltage oriented control of self-excited induction generator for wind energy system with MPPT." AIP Conference Proceedings. Vol. 1968. No. 1. AIP Publishing LLC, 2018.
[12] Bendjeddou, Yacine, et al. "Super twisting sliding mode approach applied to voltage orientated control of a stand-alone induction generator." Protection and Control of Modern Power Systems 6.1 (2021): 18.
[13] Morfín, Onofre A., et al. "The squirrel-cage induction motor model and its parameter identification via steady and dynamic tests." Electric Power Components and Systems 46.3 (2018): 302-315.
[14] Levi, E. "Modelling of saturated induction machines using flux linkages as state variables." Proceedings of the International Power Engineering Conference IPEC. Vol. 95. 1995.
[15] Ors, Marton. "Voltage control of a self-excited induction generator." 2008 IEEE International Conference on Automation, Quality and Testing, Robotics. Vol. 3. IEEE, 2008.
[16] H. Gharsallaoui, M. Ayadi, M. Benrejeb and P. Borne (2009), 'Flatness-based Control and Conventional RST Polynomial Control of a Thermal Process', Int. J. of Computers, Communications & Control, vol. IV, no. 1, pp. 41-56.
[17] Senoussaoui, Abderrahmene, et al. "LQGi/LTR controller with integrators and feedforward controller applied to a Twin Rotor MIMO System." Przegląd Elektrotechniczny 97 (2021).